Biochem. J. (1991) 279, 883–890 (Printed in Great Britain)



# p52(PAI-1) and actin expression in butyrate-induced flat revertants of v-*ras*-transformed rat kidney cells

Paul J. HIGGINS and Michael P. RYAN
Department of Microbiology and Immunology, Albany Medical College, 47 New Scotland Avenue, Albany, NY 12208, U.S.A.

Flat revertants of v-*ras*-transformed (KNRK) rat kidney cells, which express elevated levels of p21*ras* protein, were generated to high efficiencies with sodium butyrate (NaB). Overall protein synthesis in revertants was not different from parental cells, although changes were evident in expression and distribution of specific microfilament-associated cytoskeletal proteins. Quantitative two-dimensional electrophoresis revealed revertant-associated 3–4-fold increases in cytoskeletal deposition of the microfilament-associated proteins gelsolin and vinculin correlating with microfilament reorganization and focal-contact formation respectively. Similar increases in actin content were evident at both the total-cellular- and cytoskeletal-associated-protein levels. In contrast, intermediate-filament family elements (vimentin, lamins) remained unaltered. The only unique protein resolved in flat revertants was p52, a 52 kDa extracellular-matrix-associated protein previously identified as plasminogen-activator inhibitor type 1 (PAI-1). p52(PAI-1) expression was induced early during generation of the revertant phenotype and preceded development of focal-contact structures. NaB-induced p52(PAI-1) synthesis and generation of early morphological reversion in KNRK cells required ongoing RNA synthesis, since exposure to actinomycin D before addition of NaB inhibited both events. p52(PAI-1) induction by NaB was regulated at the level of mRNA abundance; in contrast, actin mRNA levels were the same in parental and revertant cells, suggesting that the increased actin content which typified the revertant phenotype was due to augmented actin microfilament stability.

## INTRODUCTION

Flat revertants of *ras*-oncogene-transformed fibroblasts appear morphologically 'normal', show no evidence of altered *ras* gene structure and often continue to express high levels of *ras* mRNA and p21*ras* protein (Samid *et al.*, 1987; Yamada *et al.*, 1990; Ledwith *et al.*, 1990). Morphological reversion is presumed to result from the uncoupling of particular (mediator) genes from *ras*-dependent transduction pathways (Yamada *et al.*, 1990). Since changes in cytoarchitecture and substrate adhesion typify *ras*-transformed cells (Egan *et al.*, 1987; Sistonen *et al.*, 1987; Higgins, 1989*a*,*b*), factors which regulate these processes are obvious candidate 'mediators'. Indeed, recent findings have implicated specific cytoskeletal elements and the 52 kDa extracellular-matrix-associated glycoprotein p52 in the development of phenotypic revertants (Ryan & Higgins, 1989; Higgins & Ryan, 1989). p52 has been identified as plasminogen-activator inhibitor type-1 (PAI-1) (Higgins *et al.*, 1990), a regulator of extracellular urokinase–plasminogen activator (Pollanen *et al.*, 1987, 1988) and, thereby, of pericellular proteolysis (Laiho *et al.*, 1987; Laiho & Keski-Oja, 1989). Rat fibroblasts transformed with the retroviral v-K-*ras* or human EJ*ras*$^{val\text{-}12}$ oncogenes are deficient in p52(PAI-1) (referred to hereafter as 'p52') expression (Cohen *et al.*, 1989; Ryan & Higgins, 1989; Higgins & Ryan, 1989; Higgins *et al.*, 1990; Newman *et al.*, 1990). This deficiency might contribute to the pleomorphic shape and motile behaviour of *ras*-transformants as butyrate-(NaB)-induced flat reversion requires p52 re-expression and its extracellular matrix deposition (Ryan & Higgins, 1988, 1989; Higgins & Ryan, 1989). Specific cell-to-matrix adhesive structures (i.e. focal contacts), and associated cytoskeletal elements, are affected by NaB (Altenburg *et al.*, 1976). It is not known, however, to what extent the complement of cytoskeletal proteins reflects generation of the revertant phenotype, nor at which levels changes in gene expression for the major participating elements (i.e. p52, actin) are actually regulated. These issues are addressed in the present paper.

## MATERIALS AND METHODS

### Cell culture, metabolic labelling and extract preparation

Culture of normal rat kidney (NRK) and v-K-*ras*-transformed (KNRK) cells, derivation of flat revertants with NaB (2 mM final

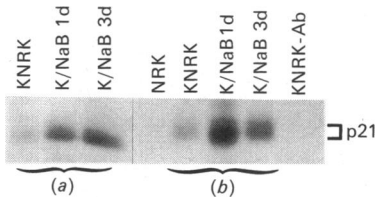


**Fig. 1. Immunoprecipitation of p21*ras* from KNRK cells and NaB-induced flat revertants (K/NaB)**

Cells were labelled with [$^{35}$S]methionine at high (90% confluent growth; *a*) or low (30% confluent growth; *b*) population densities. Revertants expressed considerably more immunoreactive p21*ras* than did parental KNRK cells when assayed both at early (1 day) and late (3 days) time points into generation of the flat phenotype. Very high levels of p21*ras* expression occurred at day 1 in low-cell-density cultures, correlating with extensive membrane ruffling (Fig. 2). Although NRK cells appear unreactive with the *ras*-11 antibody, low levels of p21*ras* were detected with longer exposures. Identical results were obtained with the Y13-259 and ras-11 antibodies. Substitution of normal IgG for antibodies to p21*ras* (no-antibody control) resulted in loss of immunoreactive p21*ras*.

Abbreviations used: NaB, sodium butyrate; p52(PAI-1), a 52 kDa extracellular-matrix-associated protein previously identified as plasminogen-activator inhibitor type 1; NRK, normal rat kidney cells; KNRK, v-K-*ras*-transformed kidney cells; TN, Tris/NaCl; HBSS, Hanks balanced salt solution; CMF-PBS, $Ca^{2+}$ + $Mg^{2+}$-free phosphate-buffered saline; i.e.f., isoelectric focusing; Rh, rhodamine; rPAI-1, anti-(rat PAI-1); 1 × SSC, 0.15 M-NaCl/0.015 M-sodium citrate; TM1, high-$M_r$ tropomyosin.

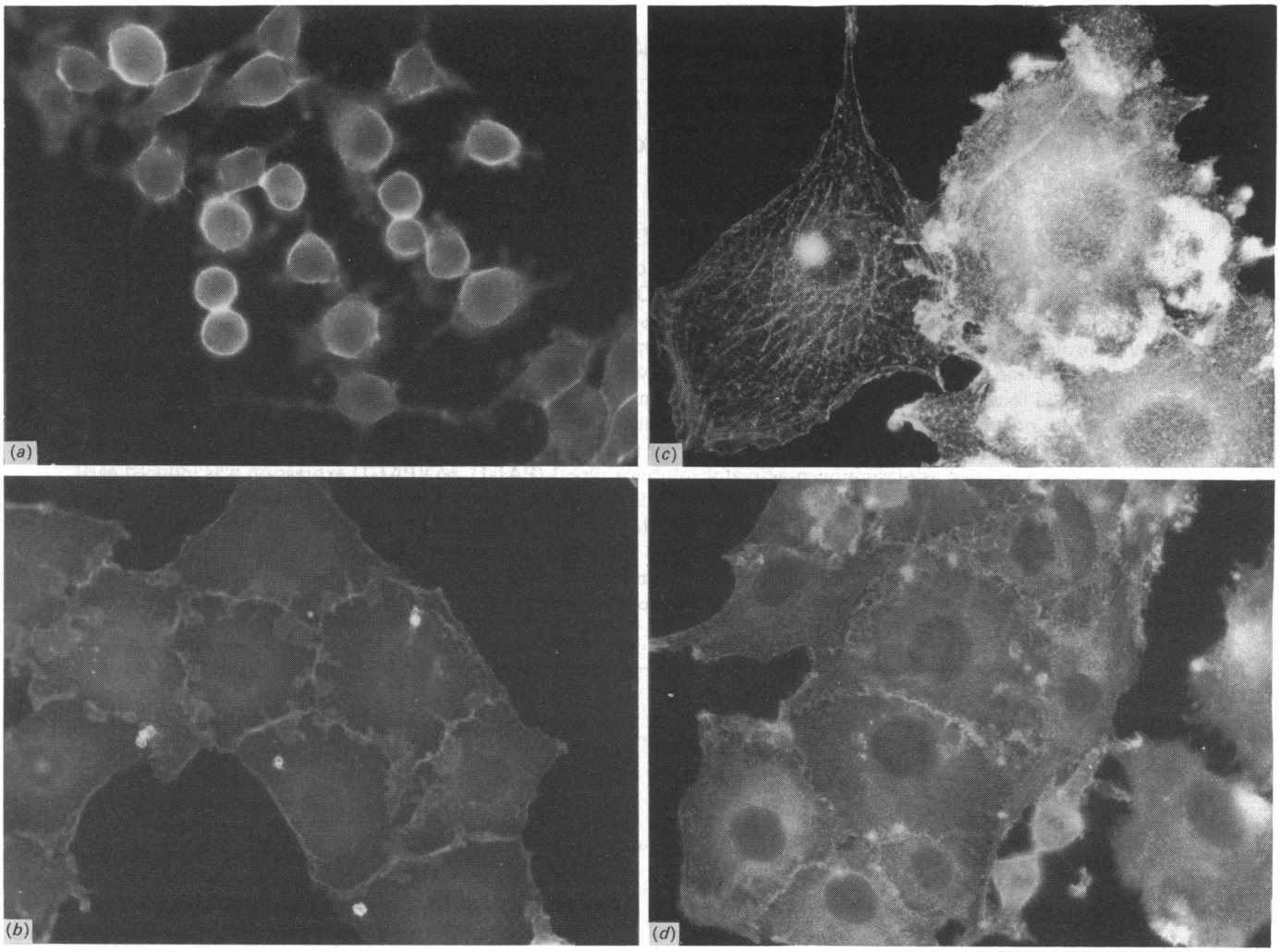


**Fig. 2. Comparative morphology and p21*ras* distribution in KNRK cells and revertants**

(*a*) p21*ras* in the typically rounded- to spindle-shaped KNRK cell population was plasma-membrane-associated, but variable in cell-to-cell distribution. In 3–5-day-NaB-treated revertants (*b*), p21*ras* was still restricted to the plasma membrane and, in particular, to ruffling edges between cells, but was quite uniform in cell-to-cell distribution. These same ruffling structures bound Rh–phalloidin (*d*), indicating the presence of F-actin in these membraneous regions. Intense ruffling occurred in KNRK cells on day 1 after NaB addition when NaB was added to low-cell-density (30% confluent growth) cultures (*c*). (*a* and *b*) p21*ras* immunofluorescence microscopy; (*c* and *d*) Rh–phalloidin-stained F-actin structures. In (*c*), one flattening cell with a well-developed MF network (rare for this early time point) and a cell with extensive ruffling activity are evident. In (*d*), focus is on the intercellular ruffles on the apical surface between adjacent cells.

concn.), labelling with [$^{35}$S]methionine (sp. radioactivity 1100 Ci/mmol, 50 $\mu$Ci/ml), and exposure to actinomycin D (5 $\mu$g/ml) and cytochalasin D (0.1 mM) were as described by Ryan & Higgins (1988) and Higgins *et al.* (1989, 1990, 1991). To inhibit *N*-linked glycosylation, tunicamycin was added (0.25–2.0 $\mu$g/ml final concn.) to the medium 24 h before, and during, metabolic labelling, after which the medium, containing secreted proteins, was aspirated and clarified at 13000 ***g***. For preparation of cytoskeletal fractions, Hanks-balanced-salt-solution (HBSS)-washed monolayers were extracted at 4 °C for 5 min in Tris/NaCl (TN)/Triton buffer [140 mM-NaCl/10 mM-Tris/HCl (pH 7.6)/1% Triton X-100] (Higgins, 1989*b*), the extract buffer removed, and the cytoskeletal residue scraped into TN/Triton buffer, vortex-mixed, and collected at 13000 ***g***. Cytoskeletal proteins were solubilized in first-dimension buffer (9.8 M-urea/2% Nonidet P40/2% pH 7–9 ampholytes/100 mM-dithiothreitol) (Ryan & Higgins, 1988). Total cell lysates were prepared directly in first-dimension buffer. For analysis of the saponin-resistant fraction [comprising focal-contact structures and the associated undersurface proteins (Neyfakh & Svitkina, 1983)], monolayers were washed with $Ca^{2+}+Mg^{2+}$-free phosphate-buffered saline (CMF-PBS; 140 mM-NaCl/10 mM-sodium phosphate, pH 7.1), then incubated at 25 °C in 0.2% (w/v) saponin/CMF-PBS for 20 min with gentle rocking (Higgins *et al.*, 1989). Cells were dislodged with a stream of CMF-PBS, and the substrate-attached residue (saponin fraction) was scraped into first-dimension-PAGE sample buffer (below).

### One- and two-dimensional PAGE

[$^{35}$S]Methionine-labelled trichloroacetic acid-insoluble total cellular or cytoskeletal proteins ($5\times10^5$–$2\times10^6$ c.p.m.) in first-dimension buffer were separated by isoelectric focusing (i.e.f.) on pre-run 1.5-mm-diameter tube gels (pH 5–7/3–10 ampholytes, 5:1, v/v) before separation by molecular mass on SDS/10%-acrylamide slab gels (Ryan & Higgins, 1988; Ryan *et al.*, 1989). One-dimensional PAGE of 25000 c.p.m. of secreted and saponin-fraction protein was as described by Ryan & Higgins, 1988,

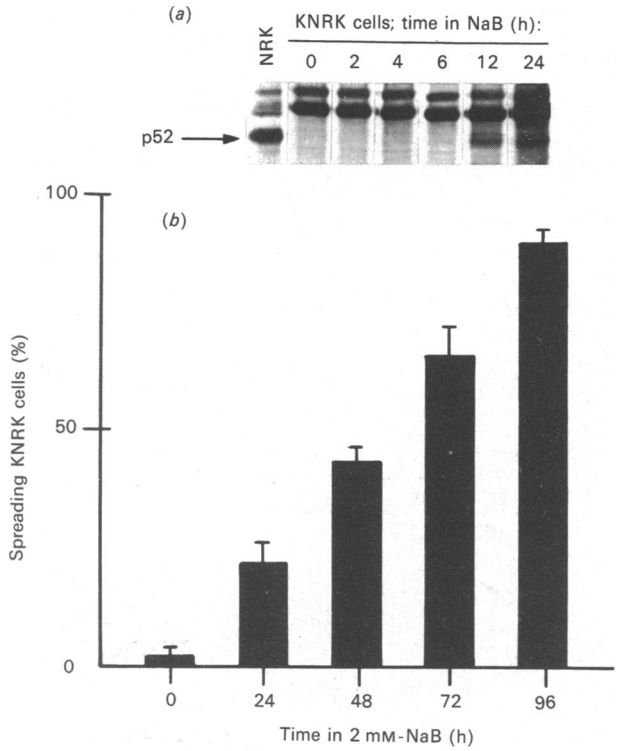


**Fig. 3. Accumulation of p52 in NaB-treated KNRK-cell cultures occurred within 6–12 h after initial exposure to NaB (*a*) and prior to the onset of increased cell spreading (*b*)**

The secreted protein fraction of NRK cells provided an internal p52 standard (arrow). The percentage of spreading cells was assessed by phase-contrast microscopy. Results are means ± S.D. for triplicate determinations on three random sets of 100 cells each.

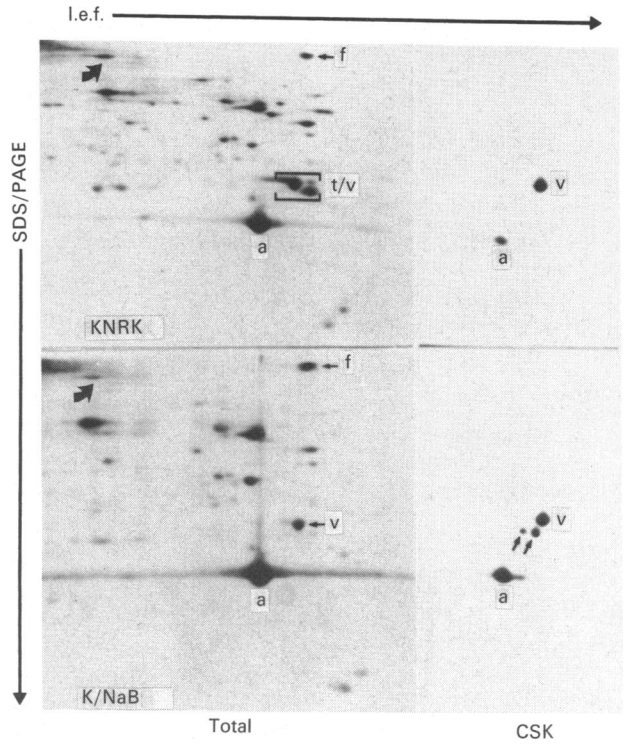


**Fig. 4. Two-dimensional gel-electrophoretic profile of [$^{35}$S]methionine-labelled total cellular protein ($5 \times 10^5$ c.p.m.; left panels) or actin/vimentin-region cytoskeletal (CSK) proteins ($1 \times 10^5$ c.p.m.; right panels) from parental KNRK (top) and NaB-treated (K/NaB) revertant (bottom) cells**

Evident are revertant-associated increases in both total cellular and cytoskeletal actin (a) content; vimentin (v) levels are the same in both cell types, while tubulin (t) is considerably decreased. Two cytoskeletal 55 kDa proteins expressed at high level in revertants (unlabelled arrows; bottom right panel) correspond to rat granulosa-cell proteins 1/2 (Ben-Ze'ev & Amsterdam, 1987). The thick arrow designates vinculin; fibronectin (f) and tubulin/vimentin (t/v) are indicated.

1989). Labelled proteins were revealed by fluorography and quantified (as a function of c.p.m. loaded) with a Zeiss MOPS III digital image analyser (Higgins & Ryan, 1989). Proteins were identified by pI/$M_r$, by computer-based spot-set matching with a two-dimensional gel Scanalyzer (CSI, Beillerica, MA, U.S.A.) according to the REF52 Database (Garrels, 1989; Garrels & Franza, 1989) or by immunoblotting using specific antisera (Higgins *et al.*, 1990).

### Morphology assessments and immunofluorescence microscopy

For morphological examination, cells were fixed *in situ* with 100% methanol for 10 min, then stained with Giemsa stain (Ryan *et al.*, 1987). Microfilament structures were resolved in 10%-(v/v)-formalin/PBS-fixed 1%-Nonidet P40/PBS-extracted cells with the F-actin probe rhodamine (Rh)-labelled phalloidin (Ryan & Higgins, 1988). Immunocytochemical localization of vinculin utilized the monoclonal antibody VIN-11-5 and 10%-formalin-fixed, 0.5%-Triton X-100-extracted cell cultures [all reagents were prepared in modified HBSS (i.e. HBSS without $CaCl_2$ and $MgSO_4,7H_2O$ and containing 2 mM-EGTA, 5.5 mM-$MgCl_2$ and 5 mM-Pipes)] (Higgins & Ryan, 1989). For detection of p52, PBS-rinsed methanol-fixed cells or saponin-prepared matrices were incubated in mouse anti-p52 (1:20; generated by injection of protein gel slices intraperitoneally into BALB/c mice) or rabbit anti-(rat PAI-1) (rPAI-1) (1:50; Higgins *et al.*, 1990) sera. After 2 h at 22 °C, monolayers were PBS-washed, incubated in Rh-labelled goat anti-mouse or anti-rabbit IgG (1:20) for 1 h, then washed again. Antisera specificity was ascertained by immunoprecipitation (Higgins *et al.*, 1990). p21*ras* in 10%-formalin/PBS-fixed methanol-extracted cells was localized with the monoclonal antibody *ras*-11 (New England Nuclear, Boston, MA, U.S.A.) (1:10) as described (Furth *et al.*, 1982).

**Table 1. Uptake and incorporation of [$^{35}$S]methionine into cellular protein by KNRK and revertant cells**

| Cell type | Cellular label incorporated (%)* | | Total cellular label‡ | TCA-insoluble label‡ |
|---|---|---|---|---|
| | Low density† | High density† | | |
| KNRK | 92.9 | 77.2 | 1.00 | 1.00 |
| Revertant | 83.7 | 77.9 | 0.94 | 0.85 |

* Cellular [$^{35}$S]methionine converted into trichloroacetic acid (TCA)-insoluble protein.

† Cultures labelled at 30–50% (low population density) or 90–95% (high population density) confluent growth.

‡ Relative to KNRK cells; calculated per $10^6$ cells. In additional experiments, cycloheximide ($5 \times 10^{-5}$ M final concn. added 1 h before labelling), which effectively inhibited > 95% of protein synthesis in both control and revertant cells, was used to calculate methionine pool size (by subtraction of trichloroacetic acid-insoluble c.p.m. from non-cycloheximide-treated cells from total cellular c.p.m. of cycloheximide-treated cells). No difference in methionine pool size was evident between the two cell types.

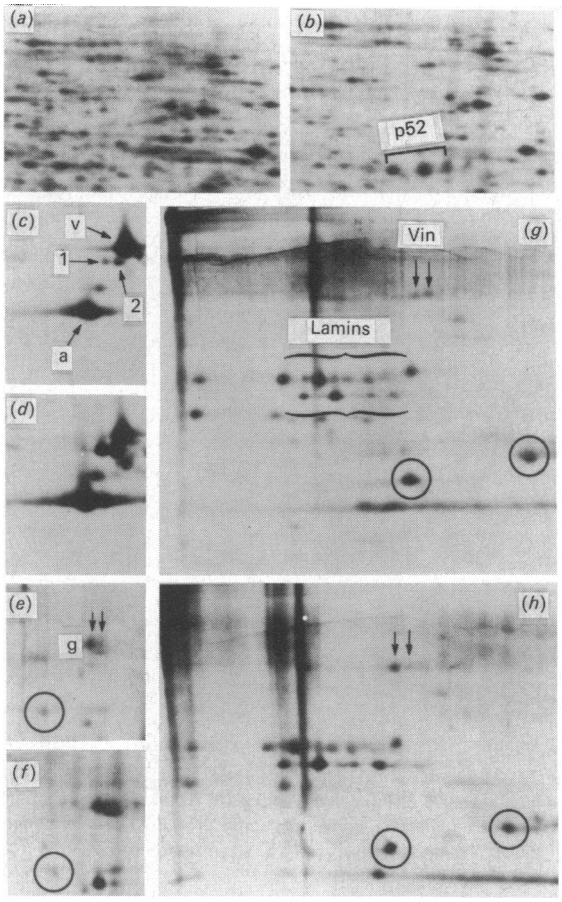


**Fig. 5. Specific differences in the cellular and cytoskeletal protein composition of parental and revertant cells**

Only relevant areas of two-dimensional gels comparing KNRK (*a*, *c*, *e*, *g*) and revertant (*b*, *d*, *f*, *h*) proteins are shown. Matched-set analysis of paired gels revealed clear revertant-associated increases in p52 (*a*, *b*) actin (a) and reference proteins 1/2 (*c*, *d*). Gelsolin (g) in parental cells (*e*) focused as two distinct isoforms, with the basic variant predominant; the greater levels of cytoskeletal gelsolin in revertants (*f*) involved increases in both isoforms. Whereas total cellular levels of vinculin (Vin) were not altered between the two cell types (Fig. 2), differences in cytoskeletal vinculin isoform distribution distinguished parental (*g*) from NaB-treated (*h*) cells. Circles (*e*, *f*, *g*, *h*) specify proteins which are expressed at similar levels in KNRK and revertant cells. Lamins A (upper) and C (lower) are indicated.

### RNA extraction, plasmid preparation and slot-blot hybridization

Total cytoplasmic RNA was isolated as detailed by Favaloro *et al.* (1980) and ribosomal RNA quantified by agarose-gel electrophoresis, followed by staining with ethidium bromide. RNAs were slot-blotted to nitrocellulose in 20 × SSC (Davis *et al.*, 1986) in triplicate sets of 20, 10 and 5 μg of RNA/slot and the filters vacuum-baked at 80 °C for 4 h. Plasmids for hybridization included pSS1–3, containing a 1.2 kb p52(PAI-1) cDNA insert in the pBSK(−) vector (Higgins *et al.*, 1990; Zeheb & Gelehrter, 1988), pBSK(−) vector without insert, and the mouse β-actin cDNA probe pActin (a gift from Dr. J. Schaeffer, New York State Department of Health, Albany, NY, U.S.A.). Endonuclease-*Eco*RI-linearized plasmids were labelled with [$^{32}$P]dCTP by random primer extension and separated free from unincorporated label on Nick Columns (Pharmacia LKB, Piscataway, NJ, U.S.A.). Hybridization conditions and washing of blots were as described by Higgins *et al.* (1990).

### Immunoprecipitation of p21*ras*

[$^{35}$S]Methionine-labelled cells were washed twice with PBS and lysed in 200 μl of immunoprecipitation buffer (10 mM-Tris/HCl/0.15 M-NaCl/1 % Triton X-100/0.5 % deoxycholate/0.1 % SDS) (Higgins *et al.*, 1986). Lysates were clarified at 13000 *g*, and $5 \times 10^6$ c.p.m. of trichloroacetic acid-insoluble protein were diluted to a final volume of 200 μl before addition of 5 μl of Y13-259 (gift of Dr. M. Furth, Sloan-Kettering Institute, New York, NY, U.S.A.) or 10 μl of *ras*-11 antibodies. Immunoprecipitation was done as described by Furth *et al.* (1982), but using GammaBind G-agarose beads (Genex Corp., Gaithersburg, MD, U.S.A.) to collect immune complexes. After three washes in immunoprecipitation buffer, beads were resuspended in 50 μl of electrophoresis sample buffer [50 mM-Tris/HCl (pH 6.8)/10 % (v/v) glycerol/1 % (w/v) SDS/1 % (v/v) 2-mercaptoethanol], boiled for 2 min, then removed by centrifugation at 13000 *g*. Immunoprecipitated proteins were fractionated on SDS/12 %-acrylamide slab gels.

## RESULTS

### p21*ras* expression in flat revertants

Revertants not only continued to express p21*ras*, but did so at levels approx. 6–10-fold greater than that of parental cells (Fig. 1). In both cell types, p21*ras* localized exclusively to the plasma membrane, where it co-distributed with F-actin-enriched ruffles and undulations (Fig. 2). Unlike KNRK controls, in which there was considerable cell-to-cell variability in p21*ras* immunofluorescence intensity, revertants were uniform in p21*ras* distribution and fluorescence signal. Exposure of KNRK cells to NaB at low population densities (i.e. 30–50 % confluent growth) produced extensive day-1 membrane ruffling (Fig. 2), which reflected a 12–16-fold increase in p21*ras* content (Fig. 1).

### Cytoskeletal protein changes in flat revertants

Morphological reversion involved early p52 induction (within 6–12 h of initial NaB exposure) followed by time-dependent increases in both cell spreading (ultimately involving > 80 % of the total population) (Fig. 3) and cellular/cytoskeletal actin content (Fig. 4). By day 3, a point when > 60 % of the population exhibited the flat phenotype (Fig. 3), p52 isoforms were easily detected in revertant-cell extracts by their characteristic spot pattern, molecular mass (52 kDa) and pI range (6.2–5.6) (Fig. 5). Revertant-related increases in cellular/cytoskeletal actin did not simply reflect altered label utilization or [$^{35}$S]methionine pool size (Table 1). Actin, moreover, was not the only microfilament-associated protein which distinguished parental from revertant cells. Densitometric analysis revealed a revertant-specific 4–5-fold increase in cytoskeletal deposition of a protein with the pI/molecular mass co-ordinates of gelsolin (Fig. 5). KNRK gelsolin migrated as two distinct 92 kDa spots with pI values 5.4–5.6. Gelsolin in revertants also resolved as a 92 kDa pair with the pI-5.6 species the predominant contributor to the 4-fold increase in total gelsolin resolved. Subcellular distribution of a second actin-associated protein, vinculin, was more complex. KNRK cells failed to form stress fibres (Ryan & Higgins, 1988) and did not construct vinculin-containing focal contacts (Fig. 6). Formation of complex microfilament 'crowns' typified early development of the revertant phenotype and preceded vinculin deposition into streak-like peripheral focal-contact structures (Fig. 6). Vinculin-positive focal contacts first become evident after 2 days of NaB treatment; by 3 days, 30 % of morphological

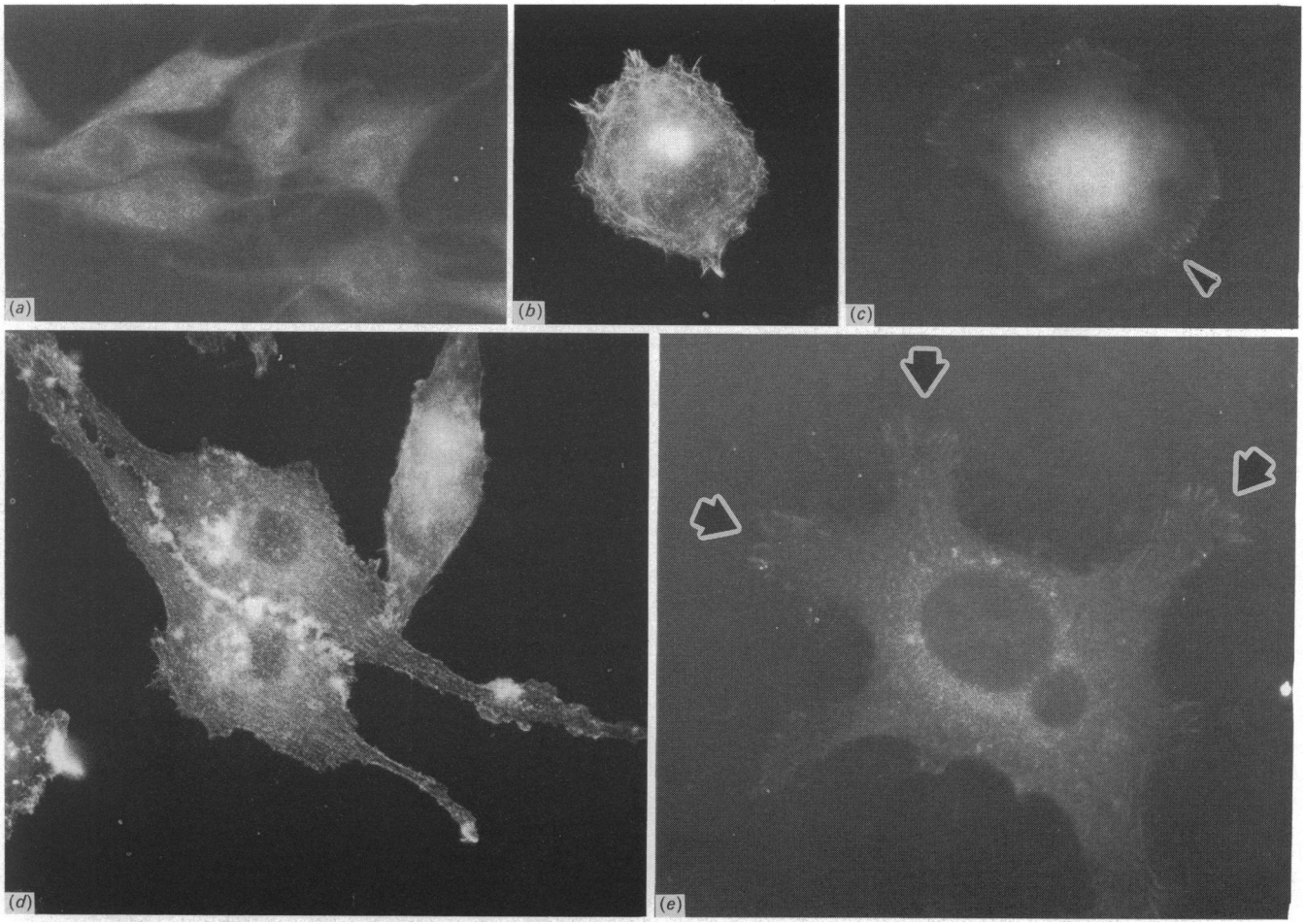


**Fig. 6. Comparative cytoarchitecture of KNRK and revertant cells**

Vinculin exhibits a diffuse cytoplasmic distribution, but no demonstrable localization to focal-contact-like elements in KNRK cells (*a*). By 2 days of NaB treatment, cells begin to flatten and develop complex peripheral microfilament arrays (*b*). Fine streak-like focal-contact structures (arrowhead) restricted to the cellular periphery are evident by day 2 of NaB treatment (*c*). At later times into development of the revertant phenotype (3–5 days), fine transcytoplasmic microfilaments are obvious in the majority of the spread cells (*d*). Cytoplasmic projections of revertant cells (arrows) are particularly enriched in focal-contact structures (*e*). (*a*), (*c*) and (*e*), Anti-vinculin immunofluorescence; (*b*) and (*d*), Rh–phalloidin fluorescence microscopy.

revertants possessed peripheral focal-contact arrays. Although there was essentially no difference in total cellular vinculin content between parental and NaB-treated cell types (Fig. 4), subcellular compartmentalization was different; revertants possessed 2.5-fold more cytoskeletal-associated vinculin than parental cells (Fig. 5). Virtually all of this increase occurred in the basic isoform of vinculin (pI 6.3) as compared with the more acidic (pI 6.1) variant. In contrast with elements comprising the microfilament network, expression of the intermediate-filament-protein family (vimentin, nuclear lamins A and C) was not changed in revertants (Fig. 5; Table 2).

### p52 in flat revertants

Unlike NRK cells, in which p52 and focal contacts distribute uniformally, both focal-contact structures and saponin-fraction p52 in revertants were restricted to the cellular periphery. Development of this vinculin-positive focal-contact ring in revertants closely correlated with the initial appearance of a 'rim' of substrate-associated p52 (Fig. 7). Time-course analysis, however, indicated that p52 was deposited into the extracellular matrix by 12–24 h after initial exposure to NaB, preceding development of the first recognizable focal contacts by at least 24 h.

Induction of p52-gene transcription by another cell-shape-modulating agent, cytochalasin D, required concomitant RNA synthesis (Higgins *et al.*, 1990). Similarly, early morphological aspects (i.e. cell spreading, microfilament reorganization) of NaB-induced reversion required RNA synthesis *de novo*, since addition of actinomycin D to KNRK cultures before NaB exposure effectively blocked the subsequent cytoarchitectural response. It was important, therefore, to determine which events were sensitive to actinomycin D blockade, as they were likely to be involved in the early morphological reorganization. Saponin-fraction proteins were selected for analysis, since saponin-residue p52 content is an important factor in NRK-cell-shape determination (Higgins *et al.*, 1991). Positive identification of p52 in the saponin fraction was required for proper assessment of actinomycin D inhibition experiments. Criteria selected included immunoreactivity with antibodies to p52/rat PAI-1, decrease in molecular mass to 43 kDa upon labelling in the presence of the *N*-linked glycosylation inhibitor tunicamycin [43 kDa is the size of the p52 'core' protein predicted by sequence analysis of both p52(PAI-1) cDNA and protein] and saponin-fraction p52 deposition (summarized in Fig. 8). No mature 52 kDa or core 43 kDa protein was secreted by KNRK cells, although both were

**Table 2. Relative content of microfilament-associated and intermediate-filament-type proteins in the cytoskeletal fraction of flat revertants**

| Protein* | Relative cytoskeletal content† (% of KNRK level)‡ |
|---|---|
| Vinculin§ | +250.9 |
| Gelsolin§ | +320.3 |
| Actin | +360.0 |
| Vimentin | −8.4¶ |
| Lamin A‖ | −5.1¶ |
| Lamin C‖ | +9.3¶ |

* Identified by pI/molecular mass (according to the REF52 Protein Database) or by immunoblotting with specific antisera.

† Assessed by quantitative densitometry of paired two-dimensional electrophoretic profiles of equivalent-c.p.m. [$^{35}$S]methionine-labelled cytoskeletal proteins of KNRK cells and NaB-induced revertants.

‡ Revertant-associated increase (+) or decrease (−) in the content of the indicated cytoskeletal protein expressed as a percentage of the corresponding KNRK cellular level. Results are means of triplicate analyses.

§ Both acidic and basic isoforms included in the assessment.

‖ Calculation based on total lamin isoforms, including differentially phosphorylated species.

¶ Differences between KNRK and revertant cells not significant.

prominent contributors to the secreted-protein complement of revertants (Fig. 8). Low levels of saponin-fraction p43 were detected in tunicamycin-treated KNRK cells (Fig. 9), approximating < 5% that of revertant populations. Since the 43 kDa p43 protein (synthesized by tunicamycin-treated NRK and revertant cells) is deposited into the saponin fraction at levels equal to that of mature p52, *N*-linked glycosylation is apparently not a major determinant in p52 targeting to the extracellular matrix. Actinomycin D effectively blocked NaB-induced p52 accumulation into both the secreted and saponin-resistant protein fractions (Fig. 9). p52 induction was similarly actinomycin D-sensitive in NaB-treated cells exposed simultaneously to cytochalasin D, a strong activator of p52-gene transcription (Chaudhari *et al.*, 1990). RNA synthesis *de novo* thus appears required for both p52 induction and the subsequent morphological reorganizational response to NaB. In contrast with p52, however, saponin-fraction actin content in actinomycin D-treated revertants was not substantially different from either non-actinomycin D-treated controls or NRK cells. This was expected, since the half-lives of actin mRNA and cytoskeletal-associated actin are significantly greater than that of p52 mRNA or saponin-fraction-associated p52 respectively (Higgins *et al.*, 1990). Whereas immunoreactive p43 was successfully translated *in vitro* using RNA from flat revertants, p43 was not detected among trans-

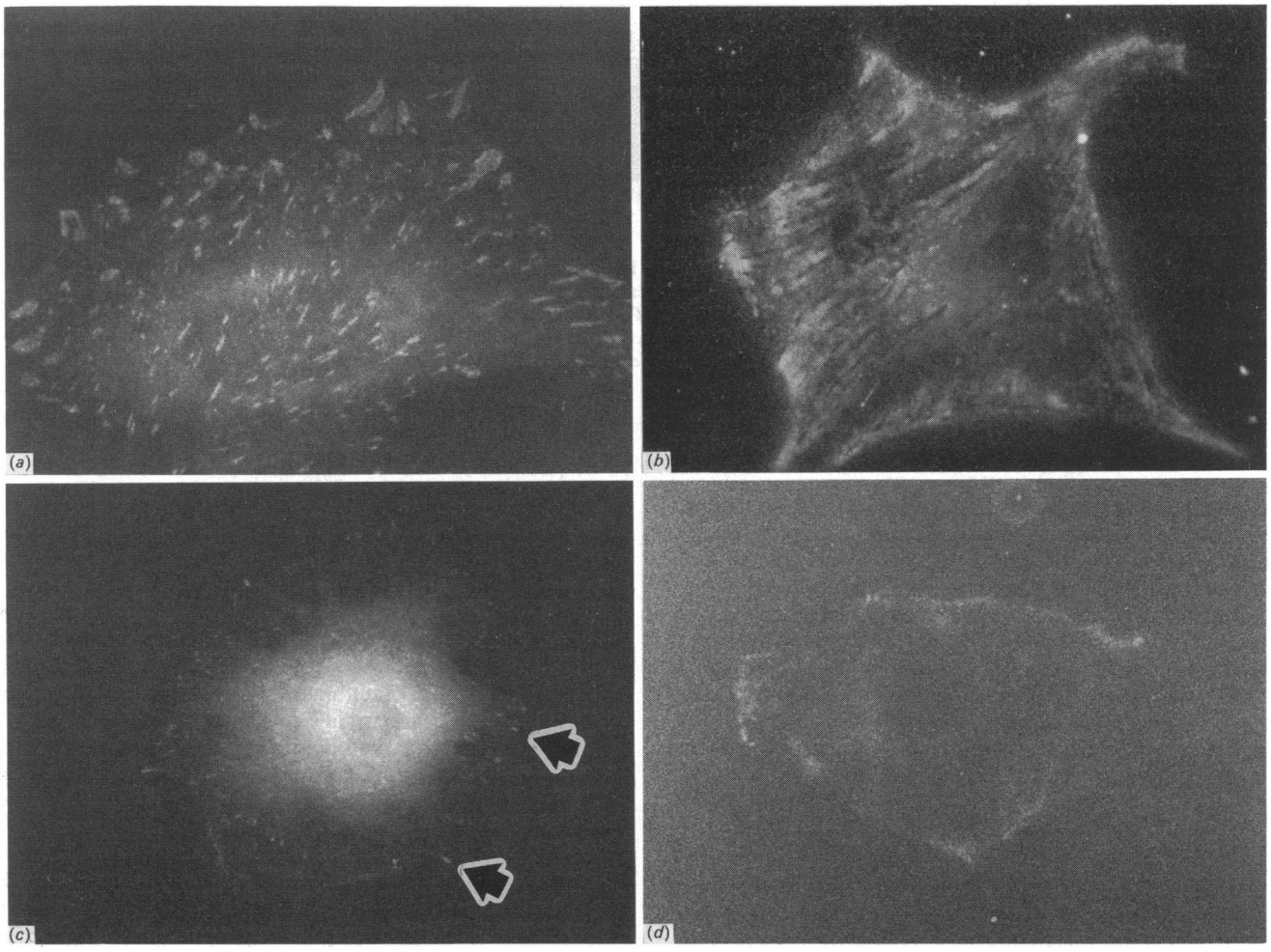


**Fig. 7. distribution of focal-contact-associated vinculin and ventral-undersurface p52 in NRK and revertant cells**

In NRK cells, typical focal-contact structures (*a*) and p52 distribute throughout the ventral cytoplasmic and undersurface regions respectively, except for obvious strial-like p52-negative areas (*b*). Focal contacts in early stage revertants, in contrast, are smaller, restricted to the cellular periphery (*c*) and co-localize with a 'rim' of ventral-undersurface-associated p52 (*d*). (*a*) and (*b*), Anti-vinculin immunofluorescence; (*b*) and (*d*), anti-PAI-1 and anti-p52 immunofluorescence respectively.

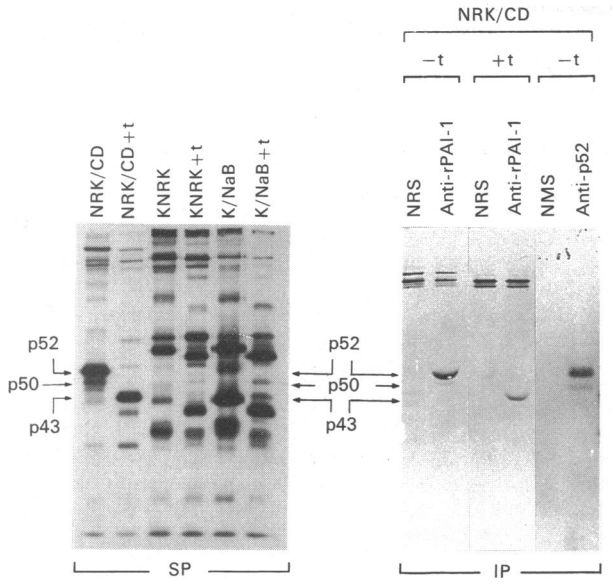


**Fig. 8. Criteria for identification of p52, p50, and p43 in one-dimensional electrophoretic separations**

Cytochalasin D-treated NRK (NRK/CD) cells and their tunicamycin(t)-treated counterparts, which accumulate significant secreted-protein-fraction levels of p52 and p43 respectively (Higgins *et al.*, 1989, 1990), provided internal p52, p50, and p43 standards (arrows). Mapping of the constituent saponin-fraction proteins by two-dimensional electrophoresis, p52 isoform analysis and identification of saponin-residue proteins in one-dimensional electrophoretic separations by concordance assignment using parallel two-dimensional maps has been described (Higgins *et al.*, 1989, 1990, 1991). p52, p50, and p43 are virtually undetectable in the secreted-protein complement of KNRK and KNRK+tunicamycin cells respectively, but are major contributors to the corresponding fraction of NaB-induced (K/NaB) flat revertants (left panel). Identification of p52, p50, and p43 was facilitated by immunoprecipitation of NRK/CD and NRK/CD+tunicamycin secreted proteins with specific antisera directed to rat PAI-1 proteins (i.e. rabbit anti-rPAI-1 and mouse anti-p52) (right panel). Normal rabbit (NRS) or mouse (NMS) sera were substituted for primary antisera in control immunoprecipitation assays. SP, secreted proteins; IP, immunoprecipitation assay.

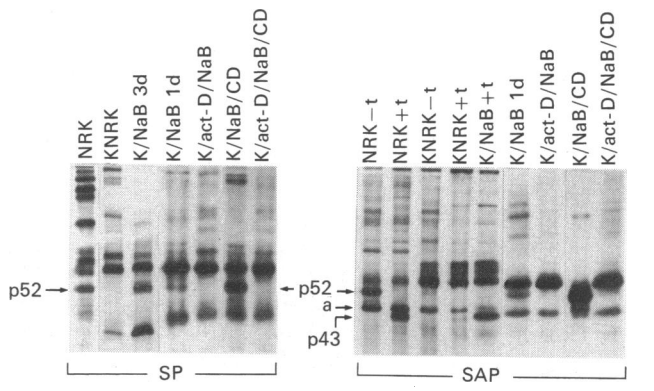


**Fig. 9. Pretreatment of KNRK cells with actinomycin D (act-D) inhibits NaB-directed p52 accumulation into both the secreted (left panel) and saponin-resistant (right panel) protein fractions**

Secreted proteins of NRK, NaB-induced revertants (K/NaB), and cytochalasin D (CD)-treated K/NaB cells provided internal p52 standards. Exposure of KNRK cells to actinomycin D before addition or NaB or NaB+cytochalasin D effectively inhibited accumulation of p52 into the secreted protein compartment (left panel). This was not simply a function of drug-induced changes in subcellular targeting or increased time of occupancy on the matrix, since actinomycin D also blocked saponin-fraction deposition of p52. Neither mature (52 kDa) nor core (43 kDa) forms of p52 could be resolved in the saponin residue of KNRK/actinomycin D cells treated with NaB or NaB+cytochalasin D (right panel). Actinomycin D therefore did not merely inhibit *N*-linked glycosylation of p52. NRK+tunicamycin (t) and K/NaB+tunicamycin cells provided internal p43 standards. SP, secreted proteins; SAP, saponin residue.

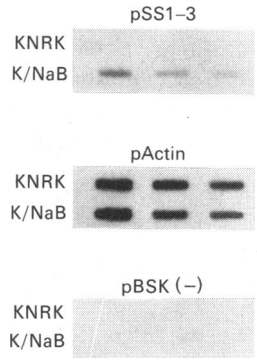


**Fig. 10. Comparison of p52 and actin mRNA abundance between KNRK cells and flat revertants (K/NaB)**

RNA was blotted to nitrocellulose in triplicate sets of 20, 10, and 5 $\mu$g/slot (left to right) and hybridized with $^{32}$P-labelled cDNAs to p52 or actin. pBSK(−) vector alone was used as a control probe. p52 mRNA was undetectable in KNRK cells, in contrast with flat revertants; no significant difference was evident in the level of actin mRNA between the two cell types.

lation products generated *in vitro* with RNA from KNRK cells (results not shown). This is consistent with the finding that RNA synthesis *de novo* is a key event in NaB-induced p52 synthesis (Fig. 9) and with hybridization data confirming the presence of p52 mRNA in NaB-treated, but not in parental, cells (Fig. 10). In contrast with p52 mRNA levels, there was no difference in actin mRNA abundance between KNRK cells and revertants.

## DISCUSSION

Several structural and regulatory elements of the actin-based microfilament network have been implicated in the cyto-architectural anomalies which typify *ras*-transformed cells (Ryan & Higgins, 1988; Higgins & Ryan, 1989). These include gelsolin (Fujita *et al.*, 1990; Banyard *et al.*, 1990), vinculin (Burridge, 1986), high-$M_r$ tropomyosin (TM1) (Matsumura *et al.*, 1983; Lin *et al.*, 1984) and actin itself (e.g. Leavitt & Kakunaga, 1980). Control of linear actin-filament assembly, moreover, is coupled to phosphatidylinositol metabolism (Stossel, 1989), which in turn appears linked to cellular *ras* activity (Yu *et al.*, 1988). Phosphatidylinositol 4,5-bisphosphate hydrolysis promotes binding of profilin to monomer actin (Lassing & Lindberg, 1988), thereby restricting actin availability for filament polymerization, and generates inositol triphosphate, which mobilizes intracellular $Ca^{2+}$ (Berridge & Galione, 1988). $Ca^{2+}$ promotes the microfilament-severing and barbed-end-blocking activities of gelsolin (Stossel, 1989), perhaps (transiently) generating a phenotype similar to that of *ras*-transformed cells. This process may be exacerbated in cell types such as KNRK, which are deficient in TM1 (Ryan & Higgins, 1988). Flow-birefringence analysis has shown that TM1 restricts the microfilament-severing action of gelsolin (Ishikawa *et al.*, 1989). Recent data, however, suggest that TM1 may not be involved in generation of the NaB-induced flat-revertant phenotype (Ryan & Higgins, 1988). Moreover, although gelsolin does sever and cap actin filaments *in vitro*, increased microfilament organization typically accompanies aug-

mented gelsolin expression in cultured cells (Banyard *et al.*, 1990; Fujita *et al.*, 1990). Apparent differences between activity *in vitro* and *in vivo* may reside in the particular variant of gelsolin and the specific cell type involved. Indeed, expression of a 92 kDa/pI 5.7 variant coincided with morphological reversion in EJ*ras*-transformed NIH 3T3/R1 cells only (Fujita *et al.*, 1990). No unique gelsolin variant was evident, however, in NaB-treated cells; a pI-5.6 isoform was constitutively expressed in KNRK cells, albeit at considerably lower levels compared with flat revertants. These data do not exclude, of course, the possibility that NaB-associated quantitative changes in gelsolin expression may underlie generation of the morphological response. It is apparent, however, that morphological reversion involves predominantly the microfilament network (and perhaps the tubulin system), since elements of the intermediate-filament-protein family were not significantly altered as a consequence of exposure to NaB.

Flat revertants generated during the course of the present study continued to express p21*ras* at levels greater than that of parental KNRK cells. p21*ras* in revertants was found in subcellular structures (i.e. ruffles, lamellar extensions) known to be typical areas of p21*ras* accumulation (Myrdal & Auersperg, 1985; Bar-Sagi & Feramisco, 1986; Bar-Sagi *et al.*, 1988). Establishment of the revertant phenotype is thus not simply a consequence of restricted expression or inappropriate targeting of the v-p21*ras* transforming protein and likely results from programmed changes in cellular gene expression. p52(PAI-1) induction and its ventral-undersurface deposition are most probably key events in this cytoarchitectural reorganization. By reducing pericellular proteolytic activity, PAI-1 may create an environment favourable for stabilization of cell-to-substrate adhesive structures. Indeed, the rim of substrate-associated p52 in revertants does co-localize with the peripheral ring of focal contacts. p52(PAI-1) distributes to the matrix as a consequence of its interaction with vitronectin, which acts to stabilize PAI-1 in an active form (Declerck *et al.*, 1988). Alternatively, PAI-1 may have other, as-yet-unrecognized, cellular functions. The subcellular distribution, relative abundance and cytoskeletal-like solubility properties of p52(PAI-1) [and PAI-1 of other species (Rheinwald *et al.*, 1987; Santaren & Bravo, 1987; White *et al.*, 1990)] suggest a potential structural role for this protein. Finally, despite the obvious difference in total cellular/cytoskeletal actin content and microfilament organization between parental and revertant cells, there was no difference in relative actin mRNA abundance. This is in obvious contrast with the early induction of p52 expression by NaB, which appears to be regulated at the level of mRNA abundance.

This work was supported by National Institutes of Health grant CA42461 and American Chemical Society Grant SIG-7A. We thank Ms. D. Higgins for manuscript preparation.

## REFERENCES

Altenburg, B. C., Via, D. P. & Steiner, S. H. (1976) Exp. Cell Res. **102**, 223–231
Banyard, M. R. C., Medveczyk, C. J. & Tellam, R. L. (1990) Exp. Cell Res. **187**, 180–183
Bar-Sagi, D. & Feramsico, J. R. (1986) Science **233**, 1061–1068
Bar-Sagi, D., Suhan, J. P., McCormick, F. & Feramsico, J. R. (1988) J. Cell Biol. **106**, 1649–1658
Ben-Ze'ev, A. & Amsterdam, A. (1987) J. Biol. Chem. **262**, 5366–5376
Berridge, M. J. & Galione, A. (1988) FASEB J. **2**, 3074–3082
Burridge, K. (1986) Cancer Rev. **4**, 18–78
Chaudhari, P. R., Ryan, M. P. & Higgins, P. J. (1990) J. Cell. Biochem. **144**, 225
Cohen, R. L., Niclas, J., Lee, W. M. F., Wun, T. C., Crowley, C. W., Levinson, A. D., Sadler, J. E. & Shuman, M. A. (1989) J. Biol. Chem. **264**, 8375–8383
Davis, L. G., Dibner, M. D. & Battey, J. F. (1986) Basic Methods in Molecular Biology, pp. 147–149, Elsevier, New York
Declerck, P. J., De Mol, M., Alessi, M.-C., Baudner, S., Paques, E.-P., Preissner, K. T., Muller-Berghaus, G. & Collen, D. (1988) J. Biol. Chem. **263**, 15454–15461
Egan, S., Weight, J. A., Jarolim, L., Yanagihara, K., Bassin, R. H. & Greenberg, A. H. (1987) Science **238**, 202–205
Favaloro, J., Treisman, R. & Kamen, R. (1980) Methods Enzymol. **65**, 718–734
Fujita, H., Suzuki, H., Kuzumaki, N., Mullauer, L., Ogiso, Y., Oda, A., Ebisawa, K., Sakurai, T., Nonomura, Y. & Kijimoto-Ochiai, S. (1990) Exp. Cell Res. **186**, 115–121
Furth, M. E., Davis, L. J., Fleurdelys, B. & Scholnick, E. M. (1982) J. Virol. **43**, 294–304
Garrels, J. I. (1989) J. Biol. Chem. **264**, 5269–5282
Garrels, J. I. & Franza, B. R. (1989) J. Biol. Chem. **264**, 5283–5298
Higgins, P. J. (1989*a*) in Cell and Molecular Biology of Colon Cancer (Augenlicht, L. H., ed.), pp. 111–138, CRC Press, Boca Raton, FL
Higgins, P. J. (1989*b*) Int. J. Biochem. **21**, 609–617
Higgins, P. J. & Ryan, M. P. (1989) Biochem. J. **257**, 173–182
Higgins, P. J., Silverstone, A. E., Bueti, C., Pizzi, V. F., Melamed, M. R., Lipkin, M. & Traganos, F. (1986) J. Natl. Cancer Inst. **76**, 885–893
Higgins, P. J., Ryan, M. P. & Chaudhari, P. (1989) J. Cell. Physiol. **139**, 407–417
Higgins, P. J., Ryan, M. P., Zeheb, R., Gelehrter, T. D. & Chaudhari, P. (1990) J. Cell. Physiol. **413**, 321–329
Higgins, P. J., Chaudhari, P. & Ryan, M. P. (1991) Biochem. J. **273**, 651–658
Ishikawa, R., Yamashiro, S. & Matsumura, F. (1989) J. Biol. Chem. **264**, 7490–7497
Laiho, M. & Keski-Oja, J. (1989) Cancer Res. **49**, 2533–2553
Laiho, M., Saksela, O. & Keski-Oja, J. (1987) J Biol. Chem. **262**, 17467–17474
Lassing, I. & Lindberg, U. (1988) J. Cell. Biochem. **37**, 255–267
Leavitt, J. & Kakunaga, T. (1980) J. Biol. Chem. **255**, 1650–1661
Ledwith, B. J., Manam, S., Kraynak, A. R., Nichols, W. W. & Bradley, M. O. (1990) Mol. Cell. Biol. **10**, 1545–1555
Lin, J. J.-C., Matsumura, F. & Yamashiro-Matsumura, S. (1984) Cancer Cells **1**, 57–64
Matsumura, F., Lin, J. J.-C., Yamashiro-Matsumura, S., Thomas, G. P. & Topp, W. C. (1983) J. Biol. Chem. **258**, 13954–13964
Myrdal, S. E. & Auersperg, N. (1985) Exp. Cell Res. **159**, 441–450
Newman, M. J., Lane, E. A., Iannotti, A. M., Nugent, M. A., Pepinsky, R. B. & Keski-Oja, J. (1990) Endocrinology (Baltimore) **126**, 2936–2946
Neyfakh, A. A. & Svitkina, T. M. (1983) Exp. Cell Res. **149**, 582–586
Pollanen, J., Saksela, O., Salonen, E.-M., Andreasen, P., Nielsen, L., Dano, K. & Vaheri, A. (1987) J. Cell Biol. **104**, 1085–1096
Pollanen, J., Hedman, K., Nielsen, L. A., Dano, K. & Vaheri, A. (1988) J. Cell Biol. **106**, 87–95
Rheinwald, J. G., Jorgensen, J. L., Hahn, W. C., Terpstra, A. J., O'Connell, T. M. & Plummer, K. K. (1987) J. Cell Biol. **104**, 263–275
Ryan, M. P. & Higgins, P. J. (1988) J. Cell. Physiol. **137**, 25–34
Ryan, M. P. & Higgins, P. J. (1989) Int. J. Biochem. **21**, 31–37
Ryan, M. P., Borenfreund, E. & Higgins, P. J. (1987) J. Natl. Cancer Inst. **79**, 555–567
Ryan, M. P., Borenfreund, E. & Higgins, P. J. (1989) Am. J. Pathol. **134**, 447–456
Samid, D., Flessate, D. M. & Friedman, R. M. (1987) Mol. Cell. Biol. **7**, 2196–2200
Santaren, J. F. & Bravo, R. (1987) Exp. Cell Res. **168**, 494–506
Sistonen, L., Keski-Oja, J., Ulmanen, I., Holtta, E., Wikgren, B. J. & Alitalo, K. (1987) Exp. Cell Res. **168**, 518–530
Stossel, T. P. (1989) J. Biol. Chem. **264**, 18261–18264
White, J. E., Tsan, M.-F., Phillips, P. G. & Higgins, P. J. (1990) Int. J. Biochem. **22**, 1159–1164
Yamada, H., Omata-Yamada, T., Wakabayashi-Ito, N., Carter, S. G. & Lengyel, P. (1990) Mol. Cell. Biol. **10**, 1822–1827
Yu, C.-L., Tsai, M.-H. & Stacey, D. W. (1988) Cell (Cambridge, Mass.) **52**, 63–71
Zeheb, R. & Gelehrter, T. D. (1988) Gene **73**, 459–468

Received 15 March 1991/17 May 1991; accepted 5 June 1991